

Author version: *Acta Geol. Sin.*, vol.87(3); 2013

**Authigenic gypsum in gas-hydrate associated sediments from the East coast of India  
(Bay of Bengal)**

M. Kocherla\*

National Institute of Oceanography, Dona Paula, Goa- 403 004, India

\* For correspondence (kocherla@nio.org)

**Abstract**

Authigenic gypsum crystals, along with pyrite and carbonate mineralization, predominantly calcites were noticed in distinct intervals in a 32 m long piston core, collected in the gas hydrate bearing sediments in the northern portion of the Krishna-Godavari basin, eastern continental margin of India in the water depths of 1691 m. X-Ray diffraction and energy dispersive spectrum studies confirm presence of pyrite, gypsum, calcite, and other mineral aggregates. The occurrence of gypsum in such deep sea environment is intriguing, because gypsum is a classical evaporite mineral and is under saturated with respect to sea water. Sedimentological, geochemical evidences point to diagenetic formation of the gypsum due to oxidation of sulphide minerals (i.e. pyrite). Euhedral, transparent gypsum crystals, with pyrite inclusions are cemented with authigenic carbonates possibly indicating that they are formed authigenically in situ in the gas hydrate influenced environment due to late burial diagenesis involving sulphate reduction and anaerobic oxidation of methane (AOM). Therefore the authigenic gypsums found in sediments of the Krishna-Godavari and Mahanadi offshore regions could be seen as one of the parameters to imply the presence of high methane flux possibly from gas hydrate at depth.

**Key words:** Authigenic gypsum, pyrites, Gas-hydrates, Krishna-Godavari and Mahanadi offshore, Anaerobic Oxidation of Methane (AOM), Eastern continental margin of India.

## 1. Introduction

Authigenic minerals and their by products are useful proxies for identifying the location of past and current natural gas hydrate occurrences and associated methane flux (Hovland et al 1987; Hovland and Judd 1988; von Rad et al 1996). In marine sediments, methane migrates upward and reacts with sulfate at the sulfate methane transition zone (SMTZ), and results in the formation of various authigenic minerals depending on the fluids, gases, and composition of the host sediments. The variety of authigenic minerals that are formed in cold seep environments provide diagnostic information on the chemistry of the diagenetic fluids, and their mineralogy, morphology and therefore can be used to indicate the magnitude of methane flux and the depth of SMTZ and consequently the presence of underlying methane gas hydrate deposits.

Sulfate is one of the major components of seawater and sulfate reduction in anoxic sediments accounts for more than 50% of the total organic carbon oxidation or mineralization (Jorgensen 1982). Moreover, sulfate also reacts with methane/ethane through sulfate reduction and anaerobic oxidation of methane (AOM) (Boetius et al 2000; Hinrichs et al 1999; Niewohner et al 1998; Hoehler et al 1994) at the sulfate methane transition zone and results in the formation of authigenic sulfide minerals depending on the pore fluid chemistry and availability of anions (Berner 1984). Pyrite is often associated with authigenic carbonates demonstrating that these minerals are by-products of sulfate reduction and methane oxidation. Pyrite formation results from the reaction of hydrogen sulfide produced by bacterial sulfate reduction with reactive iron minerals (Berner 1984; Peckmann et al 2001; Chen et al 2006). Gypsum occurrences at deep sea offshore regions are rare and uncommon. Gypsum may precipitate from rising sulfate-rich brines or due to pyrite oxidation at depth, which would flush more and more sulfate ions in to the medium and precipitates as gypsum when it exceeds the solubility concentration of gypsum (Corselli and Aghib 1987; Wang et al 2004).

The continental slope region of the K-G basin is one of the promising petroliferous basins of India. Deep sea drilling carried out in the Indian offshore region in the year 2006 during NGHP-01 expedition onboard JOIDES Resolution confirmed the presence of massive authigenic carbonates along with more than 100 m thick accumulation of massive gas hydrate deposits in the Krishna-Godavari basin, and a fully developed gas hydrate system in the

Mahanadi offshore region in the eastern continental margin of India (Collet et al 2008; Dewangan et al 2010; Mazumdar et al 2009; Ramana et al 2009; Ramana et al 2007; Kocherla et al 2006). In this paper we report a complex mixture of authigenic mineral assemblages, characterized by pyrite rich gypsum with authigenic carbonates in a 32 m long piston core collected in a water depth of 1691 m in the study area (Fig 1) and discuss their origin based on their mineralogy, morphology and its possible relationship with occurrence of sub-surface gas hydrate deposits in this part of the study area

## **2.0 Materials and Methods**

### **2.1 Sampling and core description**

A 32 m long sediment core MD-161-18 was collected on the continental slope of eastern India in the northern Krishan-Godavari (K-G) offshore basin (Lat 17°26.3106'N, Long 83°49.9501'E; water depth:1700 m) (Fig 1) on board RV Marion Dufresne (MD-161: May, 2007) using a Giant Calypso piston corer. The sedimentary sequence recovered at station MD-161-18 was divided into two lithologic units (Unit I (0-12 m) and Unit II (12-32 m) based on the authigenic mineral assemblages. Interestingly Unit I lacks authigenic minerals except small carbonate patches sporadically distributed from 7.5 to 8.5 mbsf and again reappearing as fine grained carbonate bands (~5cm thick) at deeper levels i.e. 22 mbsf (Fig 2). Sediments in Unit I (0-12 mbsf) are of silty clays while unit II (12-32 mbsf) are composed of silty clays with secondary precipitates of pyrites, gypsums and authigenic carbonates having a mean grain size of 5-7 microns. Even though four sub units were recognized within Unit II based on sedimentological criteria (On board observations, microscopic observations and variations in lithogenic, authigenic, and biogenic components as well as sedimentary structures and grain size) the entire section is considered as one unit. Water content (%) in this core narrowly varies between 38.81 and 53.80 with an average value of 43.63%. Porosity (%) varies from 59 to 74 with an average porosity of 67%. Water content and porosity in the upper sediment column (unit I) shows a gradual increase from 12 m to the core top. Down the core sediments grade into hemipelagic carbonate-poor silty clays with transitional lithologies in between, and are characterized by strong H<sub>2</sub>S smell.

### **2.2 Mineralogy of authigenic mineral assemblages**

Onboard observations and laboratory analysis of 28 sub-samples from MD-161-18 at different depths spread between 12-32 mbsf (Fig 2) showed an assemblage of authigenic gypsums along with abundant pyrite and carbonate mineralization (Fig 3). Based on onboard visual observations and lithological changes approximately 10 grams of sediment was scooped and sieved through 63 micron mesh to collect the coarse fraction. Grains of gypsum, pyrites, and carbonates were separated from the collected coarse fraction and their relative abundance (weight %) of the coarse fraction is plotted (Fig 2). Pyrite predominantly occurs at several depths and accounts for ~90% and the remaining fraction is a combination of gypsums and carbonates. All the separated mineral grains were then checked under a Nikon's SMZ-1500 binocular microscope to characterize their fabric, and morphological associations and subsequently tested by X-ray diffractometer (XRD) and by Energy Dispersive Spectrum (EDS) and as well as scanning electron microscope (SEM) to establish their mineralogy and morphology at National Institute of Oceanography, Goa India. XRD scans were done using Regaku Ultima IV X-ray diffractometer. The powdered coarse fraction (>63 micron) samples consisting of pyrite, gypsum and carbonates were run from  $10-57^{\circ} 2\theta$  at  $2^{\circ}/\text{min}$  scan speed. The individual gypsum crystals were powdered and scans were run from  $10^{\circ}-32^{\circ} 2\theta$  at  $2^{\circ}/\text{min}$  scan speed. All the above tests confirm the presence of gypsum, pyrite, and carbonates.

### **3.0 Results and discussions.**

#### **3.1 Morphological and compositional characteristics of gypsums, pyrites, and carbonates.**

Microscopic examination of 28 sub-samples at different depths spread between 12-32 mbsf showed an assemblage of euhedral authigenic gypsum crystals, micro concretions, crystal aggregates; inter growths (Figs 3,4) along with abundant pyrite and carbonate mineralization, predominantly calcite and occasionally low-mg calcite/high-mg calcite (Figs 6,7). Gypsum abundantly occurs at 12.03, 18.58, 25.01, 25.25, 25.81, 26.01, 31.04 mbsf depths. The XRD results confirmed that these crystals are gypsum minerals and have typical peaks of gypsum. The upper sedimentary sequence up to 12 mbsf lacks authigenic carbonates except small patches sporadically distributed from 7.5 to 8.5 mbsf and as fine grained carbonate bands (~5cm thick) at 22 mbsf and calcites, low-mg calcite(LMC),high-mg calcites(HMC) are amongst the carbonates. The distinct lithological boundaries in unit II is characterized by some complex

mineral assemblages (clay ball like) along with gypsums whose mineralogy could not be determined.

Morphological observations using SEM on the selected mineral aggregates show that the crystals are absolutely gypsum crystals and have clear crystal boundaries, planes, edges and cleavages of gypsum in the form either of single crystal or of twin crystals, micro concretions, crystal aggregates, inter growths (Figs 4, 5). The size of the gypsum crystals varies from few microns to 1 mm. To establish the chemical compositions these crystal aggregates were tested again by EDS. The results confirm that they were typical chemical compositions of Gypsums with Ca and S elements at almost the same atom ratio in contrast to the complex compositions to the surrounding matrix and the EDS results are presented in Table 1. Pyrites mostly occur as nodules, micro concretions (1-2 cm), thin crusts (1-2 mm) throughout the core from 12-32 mbsf and exceedingly more abundant at 25.25, 31.04 mbsf in the form of worm tubes, and chimneys (1-4 cm) respectively (Fig 7). The pyrite micro nodules are cemented with soft reddish siderite carbonates occurring as micro concretions (Fig 6c,d). The protruding nature of euhedral authigenic gypsum crystals from the surface of hard pyrite tubes are obvious (Fig 6a,b). Some pyrite tubes are black in color and coated with soft white high-Mg calcite carbonate material (Fig 6a), whereas brownish pyrite tubes are characterized by nucleation of radiating clusters of gypsum crystals (Fig 7c,e) and worm tube surfaces are with botryoidal texture (Fig 7d).

### **3.2 Origin of Gypsum and Pyrite concretions.**

Gypsum is usually formed by the evaporation on tidal flats or on still bodies of hyper-saline water or lagoons (Wells 1962; Murray 1964; Kinsman 1966; Siesser and Roger 1976). Huang and Wang et al (1994) reported its occurrence at a depth range from 200 to 1100 m in Antarctica. Yan et al (2000) reported authigenic gypsum found at a depth of 1792 m on the South China Sea. Siesser and Rogers (1976) have reported authigenic gypsum associated with pyrite in organic-rich clays in South West African continental slope. Only a few reports on authigenic gypsum are known in the regions with more than 4000 m water depth (Briskin and Schreiber 1978; Guptha et al 1980; Xavier et al 1979). Briskin and Schreiber (1978) reported authigenic gypsum on the Rio Grande Rise at a depth of 4021 m occurring as tubular gypsum

crystals growing around fragments and enclosing planktonic foraminiferal tests. Wang et al (2004) reported micro spheres of authigenic gypsum associated crystals accompanied with detrital components in Hydrate Ridge on the eastern North Pacific. Recently Pirlet et al (2009) reported diagenetic gypsum and dolomite in cold water coral mound off Ireland. Authigenic carbonates and barites were reported in gas hydrate associated sediments (Bohrmann et al 1998; Greinert et al 2001; Greinert 1999; Arrhenius 1963) but occurrence of authigenic gypsum in deep oceanic settings appears rare.

For the formation of gypsum it is essential that an overlying water or interstitial water must be rich in  $\text{SO}_4^{2-}$  ions along with an appreciable amount of  $\text{Ca}^{2+}$  ions. The  $\text{SO}_4^{2-}$  ions could be derived in three ways (i) advecting sulfate rich sea water, (ii) Organic matter decomposition and (iii) oxidation of sulfide minerals. At the oceanic bottom  $\text{SO}_4^{2-}$  could usually come from the decomposition of organic-rich sediments or oxidation of sulfides. In the present scenario the possibility of gypsum formation by evaporation or precipitation by the desiccation of interstitial water during the time of storage of the cores (Briskin and Schreiber 1978; Arrhenius 1963) could be ruled out. Desiccation can take place only when sediments are saturated with enough pore waters which can release needed amounts of dissolved sulphate from pore water for the gypsum to form (The average sea water  $\text{SO}_4^{2-}$  concentrations are about 28.8 mM and are under saturated with respect to gypsum). If this is the case gypsum could have been noticed in the upper part of the sedimentary section, but on the contrary the sedimentary section up to a depth of upper 5 mbsf does not show any gypsum thus ruling out the possibility of precipitation by desiccation. Second evidence comes from the immediate on board examination of sediments revealed sand-sized gypsum crystals (Fig 3). The above observations clearly indicate that the gypsums found here are not an artifacts but authigenic in origin.

Authigenic gypsums and pyrites reported here in the eastern continental margin of India indicate that they are most probably due to dynamic interstitial water environments prevailing due to fully a developed gas hydrate system reported in this region (Collect et al 2009). But here the question is much gypsum is oxic/evaporite mineral while pyrite is an anoxic mineral, how both can occur together? In marine sediments oxic to sub-oxic conditions are usually restricted to the top few centimeters while sediments below are anoxic. Porewater studies in

this region suggest that decomposition of organic matter by sulphate reduction within upper few centimeters while sulphate reduction coupled with anaerobic oxidation of methane is constrained to the underlying sediments. Sulfides produced during sulphate reduction react with the ferric iron minerals in the siliclastic fraction and precipitates as pyrites (Berner 1984). The abundance of pyrite (Fig 2) in our data strongly supports the contention.

The co-occurrence of gypsum, and pyrite suggest that pore solutions were anoxic and highly concentrated in sulfate ion concentrations, so that the bacterial sulfate reduction could take place, producing sulfides due to iron and sulfate reduction (Wells 1962; Briskin and Schreiber 1978; Seisser and Rogers 1976; Xavier et al 1979; Guptha 1980; Jiashen et al 2004) leaving enough sulfate ions in the solutions for the gypsum to precipitate. The needed  $\text{Ca}^{2+}$  ions for the formation of gypsum could be supplied by the dissolution of calcareous tests (Suess et al 1999; Wells 1962; Briskin and Schreiber 1978; Guptha 1980) and by spilled calcium during the formation of gas hydrate below and the gypsum was precipitated once it exceeded the solubility product of  $\text{CaSO}_4$  (Suess et al 1999; Wang et al 2004; Corselli and Aghib 1987). The occurrence of anhydrite along with euhedral gypsum crystals at several subsurface depths indicate that it has increased the solubility product of gypsum triggering its precipitation within the sediments via the interstitial water because of the lower solubility products of gypsum (Huang and Wang 1994; Wang et al 2004).

Additional supporting evidence comes from the highly depleted stable isotopic compositions of authigenic carbonate precipitates ( $\delta^{13}\text{C} = -44.83$  VPDB) that occur along with pyrites and gypsums. Methane derived authigenic carbonate with pyrite associations have been reported by several workers (Berner 1984; Peckmann et al 2001; Chen et al 2006; Gontharet et al 2007; Kocherla et al 2006; Kocherla et al 2011, Mazumdar et al 2009). Precipitation and consequent preservation of authigenic carbonates occur mainly due to increase in bicarbonate  $[\text{HCO}_3^-]$  ion concentration in pore waters. This bicarbonate  $[\text{HCO}_3^-]$  ion is derived by coupled anaerobic methane oxidation (AOM) and sulphate reduction (Boetius et al 2000; Rodriguez et al 2000; Greinert et al 2001; Ritger et al 1987; Reeburg 1980; Iversen and Jørgensen 1985; Borowski et al 1996; Wallmann et al 1997; Aharon et al 1992). AMO derived authigenic carbonates, have been observed at numerous locations adjacent to gas seepages and pore

fluid venting (Hovland and Judd 1988; Han and Suess 1989; Hovland et al 1987; Botz et al 1988; Paull et al 1992; Roberts et al 1993; Suess and Whiticar 1989; Whiticar and Faber 1986).

Areas with high methane flux are characterized by shallow SMTZ and may be associated with methane hydrate deposits (Naehr et al 2007; Feng et al 2009; Peckmann et al 2009; Sassen et al 1998; Suess et al 2001; Leon et al 2007; Sahling et al 2008). The Krishna-Godavari basin in the eastern continental margins of India is a classical example of high methane fluxes (Ramana et al 2007; Ramana et al 2008; Kocherla et al 2006; Mazumdar et al 2009; Klauda and Sandler 2005). Kocherla et al (2006) reported carbon isotopic compositions of the methane-derived authigenic carbonates  $\delta^{13}\text{C} = -51.6$  to  $-48.8$  ‰ and Mazumdar et al (2009) reported  $\delta^{13}\text{C} = -41$  to  $-52$  ‰ and  $\delta^{18}\text{O} = 2$  to  $5$  ‰ in K-G Basin. The results reported in the study fall well within the composition range of methane derived carbonate both biogenic ( $-50$  to  $-110$ ‰ VPDB) and thermogenic methane ( $-50$  to  $-20$  ‰ VPDB) and are similar to the range recorded in methane derived carbonates from several other locations (Kulm and Suess 1990; Mazzini et al 2006; Canet et al 2006; Pierre and Fouquet 2007; Chen et al 2007). These depleted carbon isotopic compositions indicate that the carbon source for the formation of authigenic carbonates were gas hydrates below, and the carbonates were formed by the oxidation of methane. Pyrite is often associated with authigenic carbonates demonstrating that these minerals are by-products of sulfate reduction and methane oxidation. Pyrite formation results from the reaction of hydrogen sulfide, produced by bacterial sulfate reduction, with reactive iron minerals (Berner 1984).

We have carried out similar studies from 1 core in the KG basin (Site 17) and 9 cores (sites 19-27; Table 2) from the Mahanadi offshore regions for comprehensive understanding of both the regions and our findings are very similar to that of site 18. The abundance of pyrites with less amounts of gypsums and carbonates in Mahanadi offshore region suggest that bacterial sulfate reduction is very strong with less intense AOM, whereas K-G offshore sediments are dominated by authigenic carbonates with less amounts of gypsums, and pyrites suggesting the AOM is very strong (Mazumdar et al 2009; Kocherla et al 2012). The above studies suggest that the processes and factors are relatively similar to that of northern KG Basin as far as the formation of gypsum is concerned and probably due the existence of a fully established gas



hydrate system in the Mahanadi offshore region in the continental margins of India (Collet et al 2008). Therefore we attribute that the precipitation of gypsum is due to concomitant precipitation and oxidation of sulfide minerals, while authigenic carbonates are due to AOM from Gas Hydrate derived methane (Naehr et al 2007; Feng et al 2009; Peckmann et al 2009; Greinert et al 2001; Hinrichs et al 1999). High methane concentrations and AOM processes have been reported in this region (Kocherla et al 2006; Ramana et al 2007; Ramana et al 2008; Mazumdar et al 2009). Presence of methane hydrate within a depth zone of 30–160 mbsf has been reported from this region by Collett et al (2008).

In view of the fact that the gypsum crystals are euhedral, transparent ones with high amounts of pyrites and the host sediments are cemented with authigenic carbonates (Suess et al 2002) it is inferred that the gypsum crystals were formed authigenically in the gas hydrate influenced sedimentary environment due to late burial diagenesis involving coupled sulphate reduction, and anaerobic oxidation methane. The coexistence and striking authigenic morphology of gypsum crystals along with abundant pyrite worm tubes, chimneys and other inter-grown structures, with authigenic carbonate cementations supports the contention. Therefore the distinct authigenic gypsum crystals found in gas hydrate bearing sediments from gas hydrate survey area can also be used to infer the presence of sub-surface gas hydrates in an unknown marine environment. Further studies are in progress for comprehensive understanding of the process involved along this part of eastern continental margins of India.

### **Acknowledgements**

We thank Director, National Institute of Oceanography, Goa, India, for providing facilities and permission to publish this work. This research was funded by National Gas Hydrate Program (NGHP), India. I am extremely thankful and acknowledge the anonymous reviewers for their rave review. The author also thank T. Ramprasad A. Mazumdar and Durbar Ray and for their valuable inputs. Mr. Girish Prabhu and Mr. Vijay Khedekar are thanked for their help during XRD and SEM operation respectively. This is NIO contribution no...

#### 4.0 References.

- Aharon, P., Graber, E. R. Roberts, H. H., 1992. Dissolved carbon and delta c-13 anomalies in the water column caused by hydrocarbon seeps on the northwestern Gulf of Mexico slope. *Geo Marine Letters*, 12: 33–40.
- Arrhenius, G., 1963. Pelagic sediments, in: Hill, M. N (Ed), *The Sea*. Interscience Publishers New York:655-718.
- Berner, R.A., 1984. Sedimentary pyrite formation: an update. *Geochimica et Cosmochimica Acta*, 48: 605–616.
- Briskin, M., Schreiber, B. C., 1978. Authigenic gypsum in marine sediments. *Marine Geology*, 28: 37-49.
- Boetius, A., K. Ravenschlag, C. J. Schubert, D. Rickert, F. Widdel, A. Giesecke, R. Amann, B. B. Jørgensen, U. Witte, and O. Pfannkuche. 2000. A marine microbial consortium apparently mediating anaerobic oxidation of methane. *Nature*, 407:623-626.
- Borowski, W. S., Paull, C. K. Ussler, W, III., 1996. Marine porewater sulphate profiles indicate in situ methane flux from underlying gas hydrate. *Geology*, 24: 655–658.
- Botz, R., Faber, E., Whiticar, M, Brooks, J.M., 1988. Authigenic carbonates in sediments from the Gulf of Mexico. *Earth and Planetary Science Letters*, 88: 263-272.
- Bohrmann, G., Greinert, J., Suess, E., Torres, M., 1998. Authigenic carbonates from Cascadia Subduction zone and their relation to gas hydrates stability. *Geology*, 26(7): 647-650.
- Canet, C., R. M. Prol-Ledesma, E. Escobar-Briones, C. Mortera-Gutierrez, R. Lozano-Santa Cruz, C. Linares, E. Cienfuegos, and P. Morales-Puente.,2006. Mineralogical and geochemical characterization of hydrocarbon seep sediments from the Gulf of Mexico, *Marine and Petroleum Geology*, 23: 605–619.
- Chen, Y., Matsumoto, R., Paull, C. K., Ussler, W., III, Lorenson, T., Hart, P., Winters., W., 2007. Methane-derived authigenic carbonates from the northern Gulf of Mexico-MD02 Cruise. *Journal of Geochemical Exploration*, 95:1–15.
- Collett, T., Riedel, M., Cochran, J., Boswell, R., Presley, J., Kumar P., Sathe, A., Sethi, A., Lall, M., Sibal, V., 2008, *Indian National Gas Hydrate Program: Expedition 01*, Initial Reports, vol. 1, Directorate General of Hydrocarbons, New Delhi, India.
- Corselli, C., Aghib, F.S., 1987. Brine formation and gypsum precipitation in the Bannock Basin, Eastern Mediterranean. *Marine Geology*, 75: 185–199.
- Dewangan, p., Ramprasad, T., Ramana, M.V., Mazumdar, A., Desa, M., Badesab, F.K., 2010. Seabed morphology and gas venting features in the continental slope region of Krishna-Godavari basin, Bay of Bengal: Implications in the gas-hydrate exploration. *Marine and Petroleum Geology*, 27: 1628-1641.

- Duo Fu Chen, Dong Feng, Zheng Su , Zhi Guang Song , Guang Qian Chen, Lawrence M. Cathles III . 2006 Pyrite crystallization in seep carbonates at gas vent and hydrate site . *Materials Science and Engineering*, C(26): 602-605.
- Feng, D., Chen, D.F., Roberts, H.H., 2009b. Petrographic and geochemical characterization of seep carbonate from Bush Hill (GC 185) gas vent and hydrate site of the Gulf of Mexico. *Marine and Petroleum Geology*, 26:1190 –1198.
- Gontharet, S., Pierre, C., Blance-Valleron, M.-M., Rouchy, J.M., Fouquet, Y., Bayon, G., Foucher, J.P., Woodside, J., Mascle, J., The Nautinil Scientific Party 2007. Nature and origin of diagenetic carbonate crusts and concretions from mud volcanoes and pock marks of the Nile deep-sea fan (eastern Mediterranean Sea). *Deep-Sea Research II*, 54:1292-1311.
- Greinert, J., Bohrmann, G. Suess, E., 2001. Gas hydrate-associated carbonates and methane-venting at Hydrate Ridge: Classification and distribution and origin of authigenic lithologies. In: Paull, C. K. and Dillon, P. W., (Eds), *Natural gas hydrates: occurrence, distribution, and dynamics*. Geophysical Monograph, 24: 99–113.
- Greinert, J., Rezente 1999. Submarine Mineralbildungen: Abbild geochemischer Prozesse an aktiven Fluidaustrittsstellen im Aleutenund Cascadia-Akkretionskomplex, Kiel: *GEOMAR Report 87*, 59-74; 90-176.
- Guptha, M.V. S., 1980. Authigenic gypsum in a deep sea core from southeastern Arabian sea. *Journal Geological Society of India*, 21: 568-571.
- Hovland, M., Judd, A.G., 1988. In: Hovland, M., Judd, A.G.,(Eds), *Seabed pockmarks and seepages. Impact on Geology, Biology and Marine Environment*. Graham and Trotman, London.
- Hans Pirlet, Laura M., Wehrmann, Benjamin Brunner, Norberts Franks, Jan Dewancklele, David Van Rooij, Anneleen Foubert, Rudy Swennen, Lieven Naudts, Matthieu Boone, Veerle Cnudde, Jean-Pierre Henriët, 2010. Diagenetic formation of gypsum and dolomite in cold-water coral mound in the Porcupine Seabight off Ireland. *Sedimentology*, 57:786-805.
- Hinrichs, K.-U., J. M. Hayes, S. P. Sylva, P. G. Brewer, and E. F. Delong, 1999. Methane-consuming archaeobacteria in marine sediments, *Nature*, 398: 802–805.
- Hovland, M., Talbot, M., Qvale, H., Olausson, S. Aasbeg, L., 1987. Methane-related carbonate cements in pockmarks of the north Sea. *Journal of Sedimentary Petrology*, 57: 881-892.
- Han, M.W., Suess, E., 1989. Subduction-induced pore fluid venting and the formation of authigenic carbonates along the Cascadia continental margin: Implications for the global Ca-cycle. *Palaeogeography Palaeoclimatology and Palaeoecology*, 71: 97-118.
- Huang, H., Wang, H., 1994. Autogenetic gypsum in marine glacial sediments in Bransfield Strait Antarctica. *Journal of Tongji University* (in Chinese with English abstract), 22(1): 121-125.
- Hoehler, T, M., Alperin, M, J., Albert, D, B., 1994. Field and laboratory studies of methane oxidation in an anoxic marine sediment: Evidence for a methanogenic-sulfate reducer consortium; *Global Biogeochemical Cycles*, 8: 451–463.

- Iversen, N., Jørgensen, B. B., 1985. Anaerobic methane oxidation rates at the sulphate-methane transition in marine sediments from Kattegat and Skagerrak (Denmark). *Limnology and Oceanography*, 30: 944–955.
- Jorgensen, B., 1982. Mineralization of organic matter in the sea bed- the role of sulphate reduction. *Nature*, 296, 5858: 643-645.
- Kinsaman, David., 1966. Gypsum and anhydrite of recent age Trucial coast Persian Gulf. In: *Proceedings of second symposium on salt-1*.
- Kocherla, M., Mazumdar, A., Narsing Rao, A., Joao, H.M., Dayal., A.D., and Patil, D.J., Occurrence and genesis of siderite nodules from Krishna-Godavari basin, Bay of Bengal. 7<sup>th</sup> *International conference on Asian marine geology (7ICAMG)* Goa, India, October 11-14, 2011:70.
- Kocherla, M., Mazumdar, A., Karisiddaiah, S.M., Borole D.V., Ramalingeswara Rao., B., 2006. Evidences of methane derived authigenic carbonates from the sediments of the Krishna – Godavari Basin, eastern continental margin of India. *Current Science*, 91: 318– 323.
- Klauda, J. B., Sandler, S. I., Global distribution of methane hydrate in ocean sediment. *Energy Fuels* 2005, 19: 459–470.
- Kulm, L. D., Suess., E., 1990. Relationship between carbonate deposits and fluid venting, Oregon accretionary prism, *Journal of Geophysical Research*, 95: 8899–8915.
- Leon, R., Somoza, L., Medialdia, T., Gonzalez, F. J., Diaz del-Rio, V., Fernandez-Puga, M. C., Maestro, A., Mata., M. P., 2007. Sea floor features related to hydrocarbon seeps in deepwater carbonate-mud mounds of the Gulf of Cadiz: From mud flows to carbonate precipitates, *Geo Marine Letters*, 27: 237–247.
- Mazumdar, A., Dewangan, P., Joa"o, H. M., Peketi, A., Khosla, V. R., Kocherla, M., Badesab, F. K., Joshi, R. K., Roxanne, P., Ramamurty, P. B., Karisiddaiah., S. M., Patil, D. J., Dayal, A. M., Ramprasad, T., Hawkesworth, C. J., Avanzinelli, R., 2009. Evidence of paleo-cold seep activity from the Bay of Bengal offshore Inida, *Geochemistry, Geophysics, Geosystems*, 10 (6): 1-15.
- Mazzini, A., Svensen, H., Hovland, M., Planke, S., 2006. Comparison and implications from strikingly different authigenic carbonates in a Nyegga complex pockmark, G11, Norwegian Seas. *Marine Geology*, 231: 89–102.
- Murray, R. C., 1964. Origin and diagenesis of gypsum and anhydrite. *Journal of Sedimentary Petrology*, 34: 512-523.
- Naehr, T.H., Eichhubl, P., Orphan, V.J., Hovland, M., Paull, C.K., Ussler III, W., Lorenson, T.D., Greene, H.G., 2007. Authigenic carbonate formation at hydrocarbon seeps in continental margin sediments: a comparative study. *Deep Sea Research Part II: Topical Studies in Oceanography*, 54:1268–1291.
- Niew"ohner, C., Hensen, C., Kasten, S., 1998. Deep sulfate reduction completely mediated by anaerobic methane oxidation in sediments of the upwelling area off Namibia; *Geochim. Cosmochim. Acta*, 62: 455–464.

- Paull, C.K., Chanton, J.P., Neumann, A.C., Coston, J.A., Martens, C.S., 1992. Indicators of methane-derived carbonates and chemosynthetic organic carbon deposits: Examples from the Florida Escarpment. *Palaios*, 7: 361-375.
- Peckmann, J., Daniel, B., Steffen, K., 2009. Molecular fossils reveal fluid composition and flow intensity at a Cretaceous. *Geology*, 37: 847-850.
- Peckmann, J., Reimer, A., 2001. Methane – derived carbonates and authigenic pyrite from the north western black sea. *Marine Geology*, 177: 129 -150.
- Pierre, C., Fouquet, Y., 2007. Authigenic carbonates from methane seeps of the Congo deep-sea fan, *Geo Marine Letters*, 27: 249–257.
- Ramana, M.V, Ramprasad, T., Paropkar A.L, Borolei, D.V. Ramalingeswara Rao B., Karisiddaiah, S.M., Desa, M., Kocherla, M., Joao, H.M., Lokabharati .P., Maria-Judith Gonsalves., Pattan, J.N., Khadge, N.H., Prakash Babu, C., Sathe, A.V., Kumar, P., Sethi, A.K., 2009. Multidisciplinary investigations exploring indicators of gas hydrate occurrence in the Krishna–Godavari Basin offshore, east coast of India. *Geo Marine Letters*, 29: 25-38.
- Ramana, M.V, Ramprasad, T, Kamesh Raju., K.A., Desa., M., 2007, Occurrence of Gas hydrates along the continental margins of India, particularly the Krishna-Godavari offshore basin. *International Journal of Environmental Studies*, 64: 675–693.
- Reeburgh, W. S., 1980. Anaerobic methane oxidation: rate depth distribution in Skan Bay sediments. *Earth and Planetary Science Letters*, 47: 345–352.
- Ritger, S., Carson, B. Suess, E., 1987. Methane-derived authigenic carbonates formed by subduction-induced pore-water expulsion along the Oregon/Washington margin. *Geological Society of America Bulletin*, 98: 147–156.
- Rodriguez, N.M., Paull, C.K., Borowski, W., 2000. Zonation of authigenic carbonates within gas hydrate-bearing sedimentary sections on the Blake Ridge: Offshore Southeastern North America. *In: Proceedings of Ocean Drilling Program, Scientific Results*, 164: 301-312.
- Roberts, H.H., Aharon, P., Walsh, M.M., 1993. Cold-seep carbonates of the Louisiana continental slope-to-basin floor. In: Rezal, R., and Lavoie, D.L (Eds) Carbonate Micro fabrics, *Springer-Verlag*,95-104.
- Sassen, R., MacDonald, I. R., Guinasso, N. L., Joye, S, Requejo, A.G., Sweet, S. T., et al, 1998. Bacterial methane oxidation in seafloor gas hydrate: Significance to life in extreme environments. *Geology*, 26: 851 – 854.
- Sahling, H., Bohrmann, G., Spiess V.J. et al 2008. Pockmarks in the Northern Congo Fan area, SW Africa: Complex seafloor features shaped by fluid flow. *Marine Geology*, 249: 206–225.
- Seisser, W. G., Roger, J., 1976. Authigenic pyrite and gypsum in southwest African continental slope sediment, *Sedimentology*, 23: 567-577.
- Suess, E., Borhmann, G., Rickert, D., Kuhs, W.F., Torres, M.E., Trehu, A.M., and Linke, P., 2002. Properties and fabric of near-surface methane hydrates at Hydrate Ridge, Cascadia margin, in *Proceedings of the 4th International Conference on Gas Hydrates, Yokohama, Japan, May, 2002*.

- Suess, E., Torres, M. E., Bohrmann, G. et al., 2001. Sea floor methane hydrates at hydrate ridge, Cascadia margin, in *Natural Gas Hydrate: Occurrence, Distribution and Detection*, In: C. K. Paul and W. P. Dillon (Eds), *Geophysical Monographs Ser, AGU, Washington, D. C.*, 124: 87–98.
- Suess, E., Torres, M., Bohrmann, G., 1999. Gas hydrate destabilization: Enhanced dewatering, benthic material turnover and large methane plumes at the Cascadia convergent margin, *Earth and Planetary Science Letters*, 170:1-15.
- Suess, E., Whiticar, M.J., 1989. Methane-derived CO<sub>2</sub> in pore fluids expelled from the Oregon Subduction Zone. *Palaeogeography Paleoclimatology and Palaeoecology*, 71: 119-136.
- von Rad, U., Roesch, H., Berner, U., Geyh, M., Marchig, V., Schulz, H., 1996. Authigenic carbonates derived from oxidized methane vented from the Makran accretionary prism off Pakistan. *Marine Geology*, 136, 55-77.
- Wells, A. J., 1962. Recent dolomite in the Persian Gulf, *Nature*, 194: 274-275.
- Wang, J., Suess, E., Rickett, D., 2004. Authigenic gypsum found in gas hydrate-associated sediments from Hydrate Ridge, the eastern North Pacific, *Science in China Ser D. Earth Sciences*, 47: 280-288.
- Wallmann, K., 1997. Quantifying fluid flow, solute mixing, and biogeochemical turnover at cold vents of the eastern Aleutian Subduction zone. *Geochimica Cosmochimica Acta*, 61/24: 5209–5219.
- Wang, J., Suess, E., 2002. Indicators of  $\delta^{13}\text{C}$  and  $\delta^{18}\text{O}$  of gas hydrate associated sediments, *Chinese Science Bulletin*, 47(19): 1659-1663.
- Whiticar, M.J., Faber, E., 1986. Methane oxidation in sediment and water column environments — isotope evidence. *Organic Geochemistry*, 10: 759–768.
- Xavier, A., Klemm, D. D., 1979. Authigenic gypsum in deep sea manganese nodules, *Sedimentology*, 26: 307-310.
- Yan, W., Chen, Z., Wang, Y. et al., 2000. Mineralogical characteristics and mineral sedimentary sequences of core NS93-5 from the South China Sea, *Acta Mineralogical Sinica* (in Chinese with English abstract), 20(2):143-149.

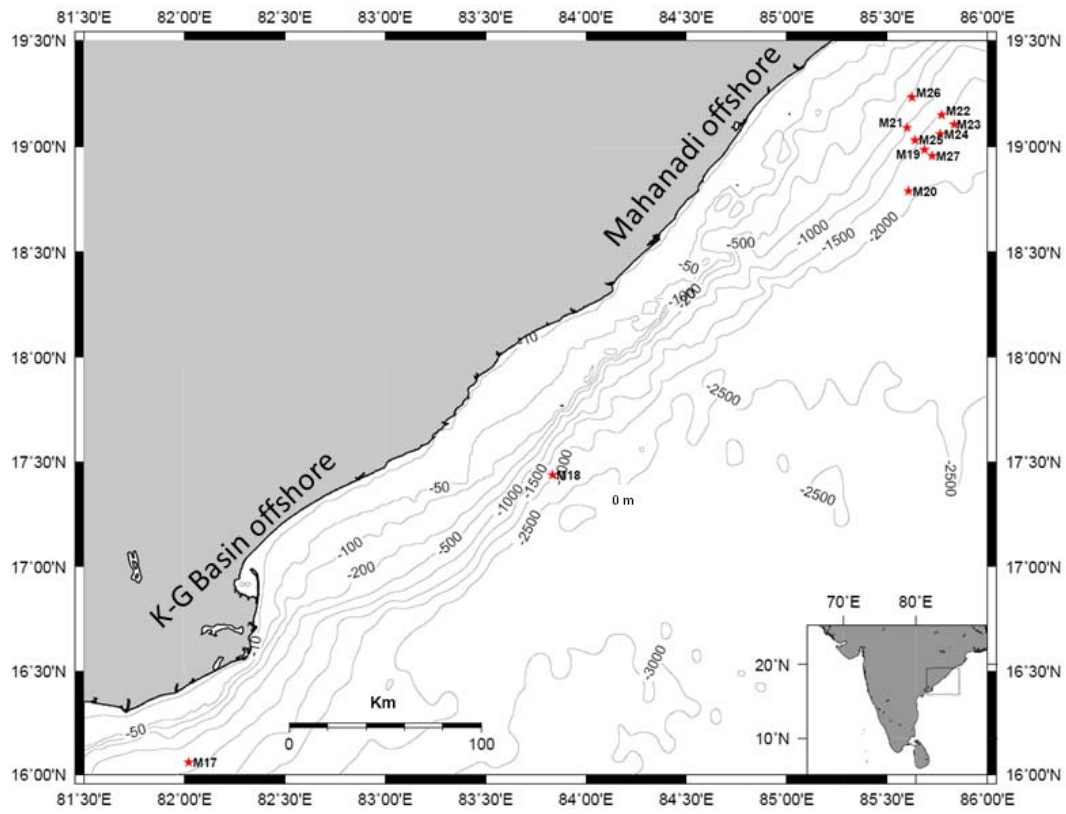


Fig.1 Core location and bathymetry map of the study area in the K-G and Mahanadi offshore region, Eastern continental margin of India

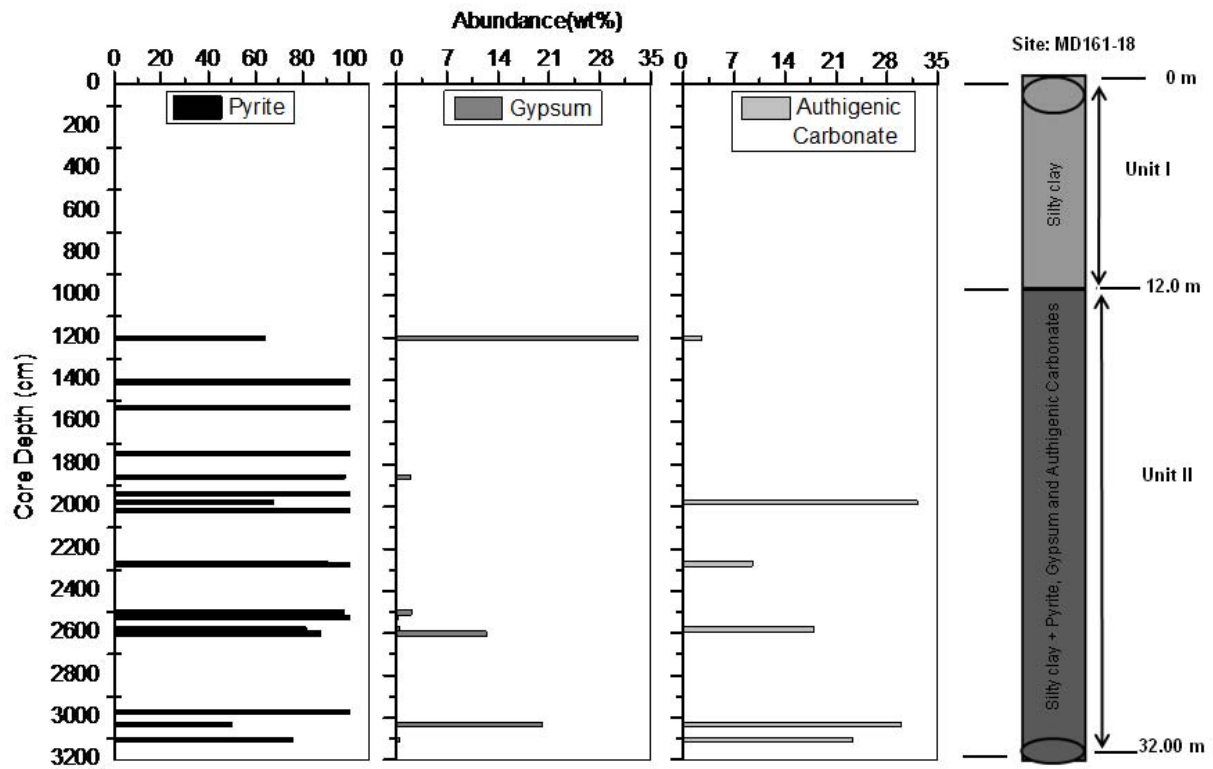


Fig.2. Bar plot showing the down core distribution and abundance of major authigenic mineral assemblages of pyrite, gypsum and authigenic carbonates along with sediment characteristics.



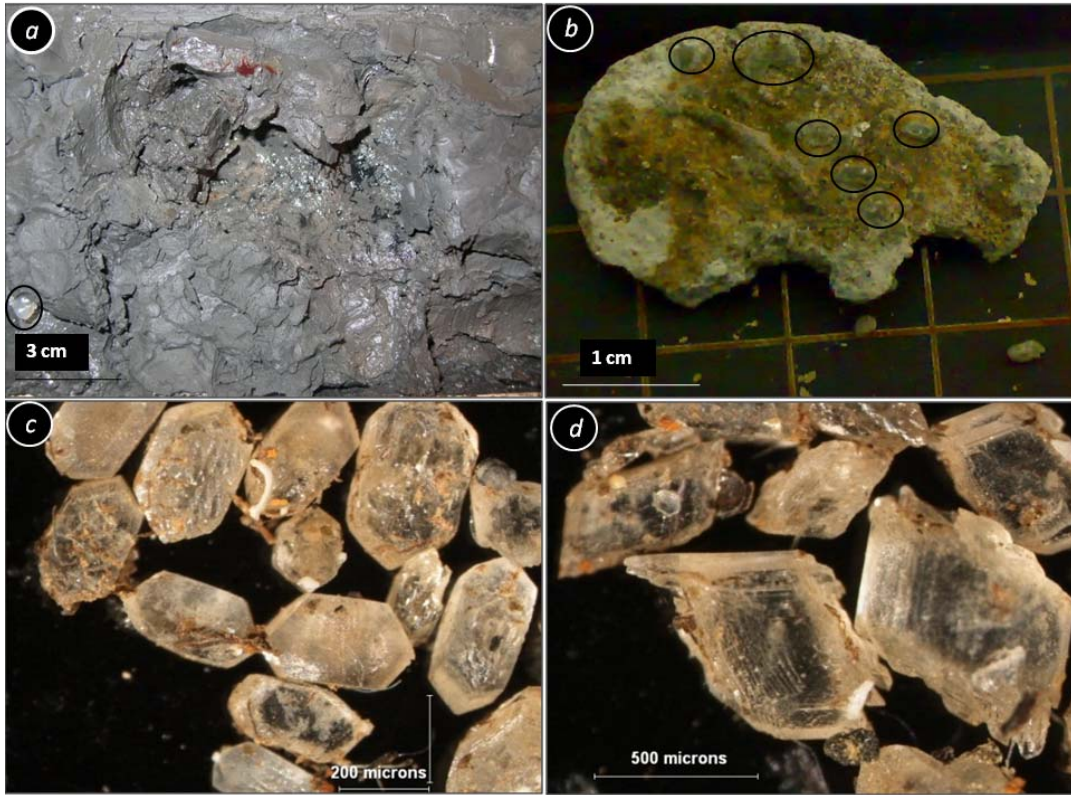


Fig.3 (a) diagenetic burrows with authigenic precipitations; (b) a slab consisting of authigenic carbonates, pyrite tubules and well developed euhedral gypsum crystals; (c) and (d) typical gypsum (selenite) crystals with lenticular shapes.

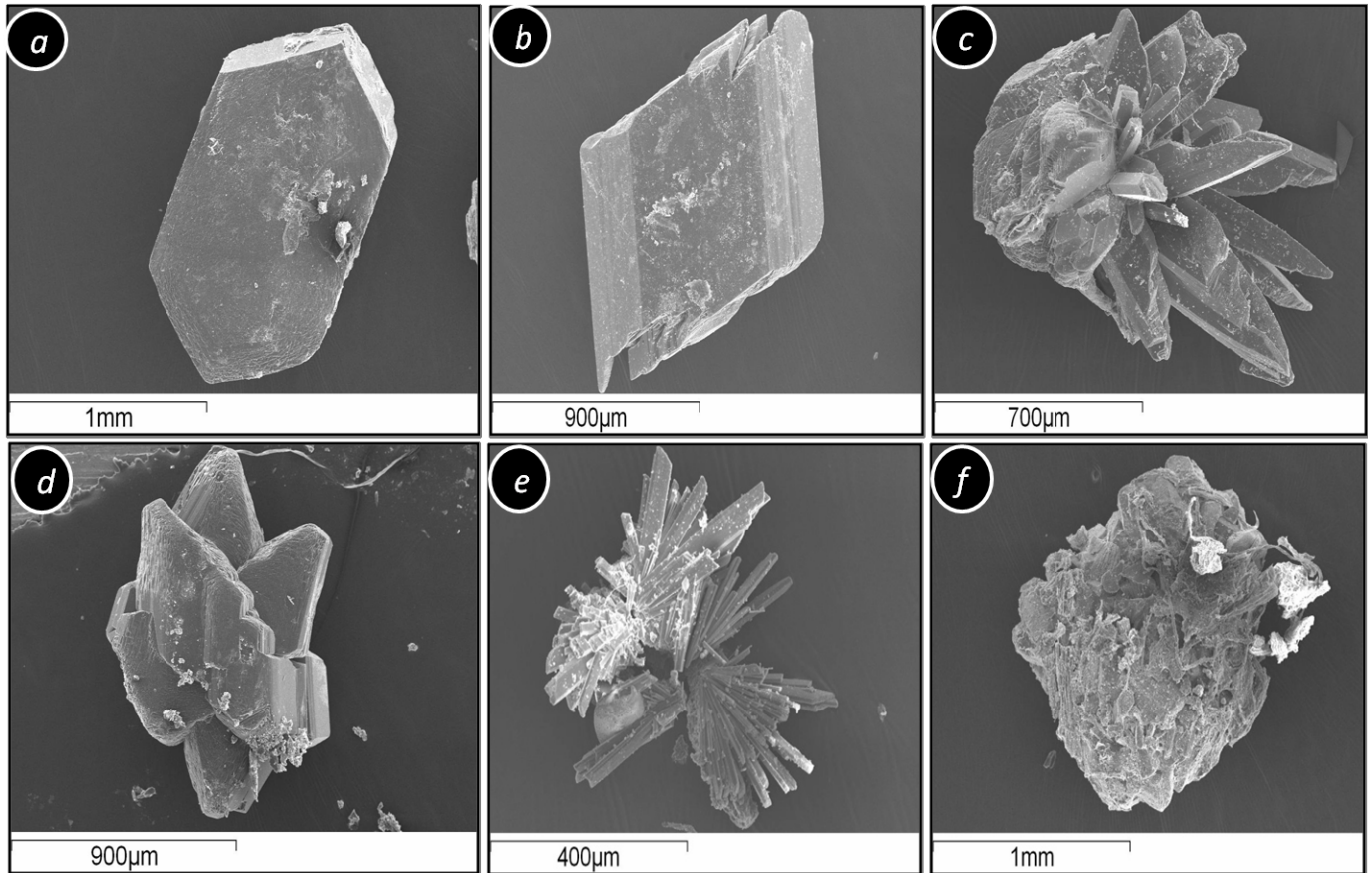


Fig.4 Scanning electron photomicrographs showing typical characteristics of gypsum crystals. (a) gypsum (selenite) with lenticular shape;(b) gypsum (selenite) variety;(c) rosette of gypsum (d) intergrowths of gypsum crystals;(e) cluster of bladed gypsum crystals;(f) complex aggregates gypsum.

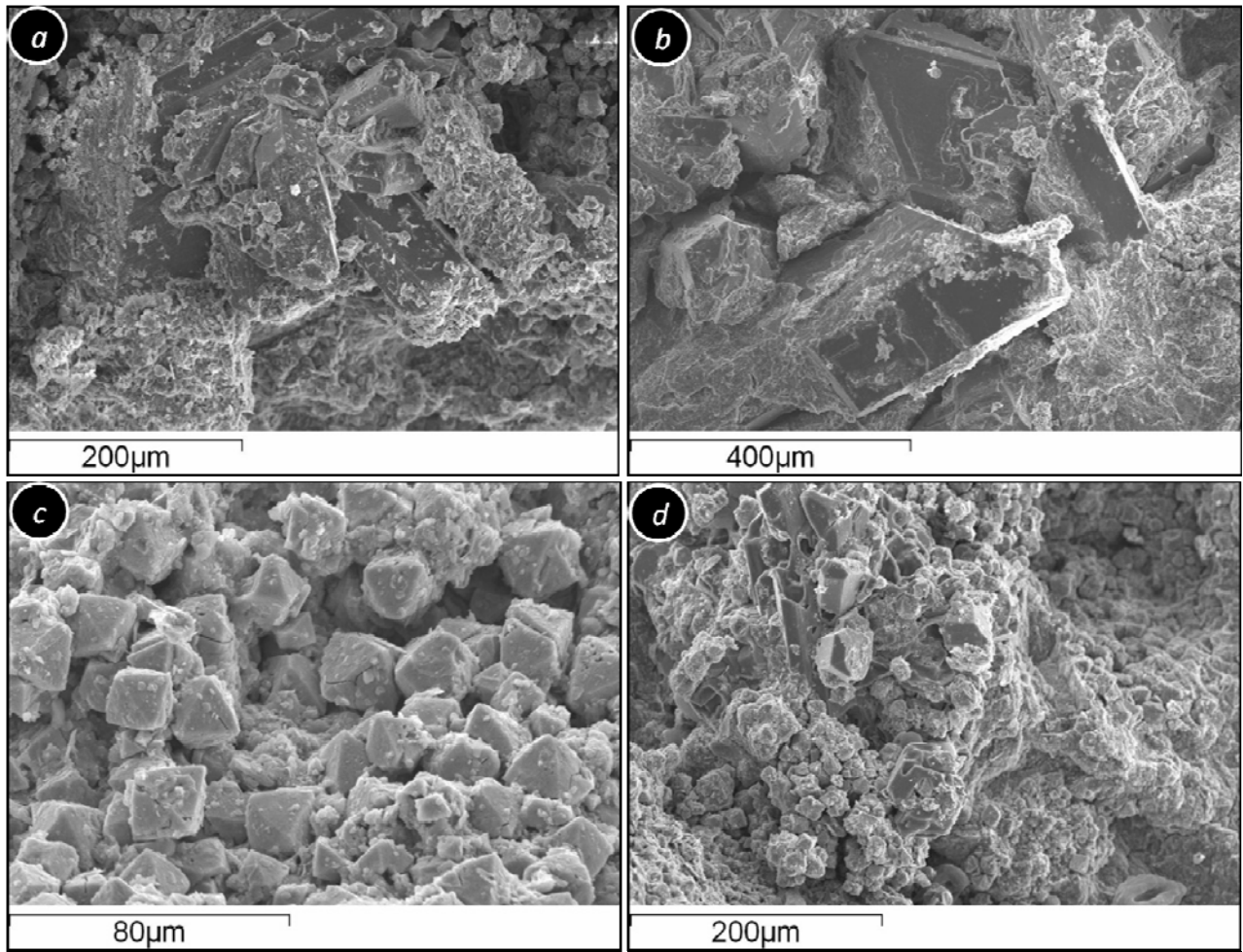


Fig.5. (a) and (b) scanning electron photomicrographs showing concomitant precipitation of gypsum crystals with lenticular shapes; (c) cubical pyrite crystals in anaerobic sediments; (d) co-occurrence of gypsum and pyrite with authigenic carbonate cementation.

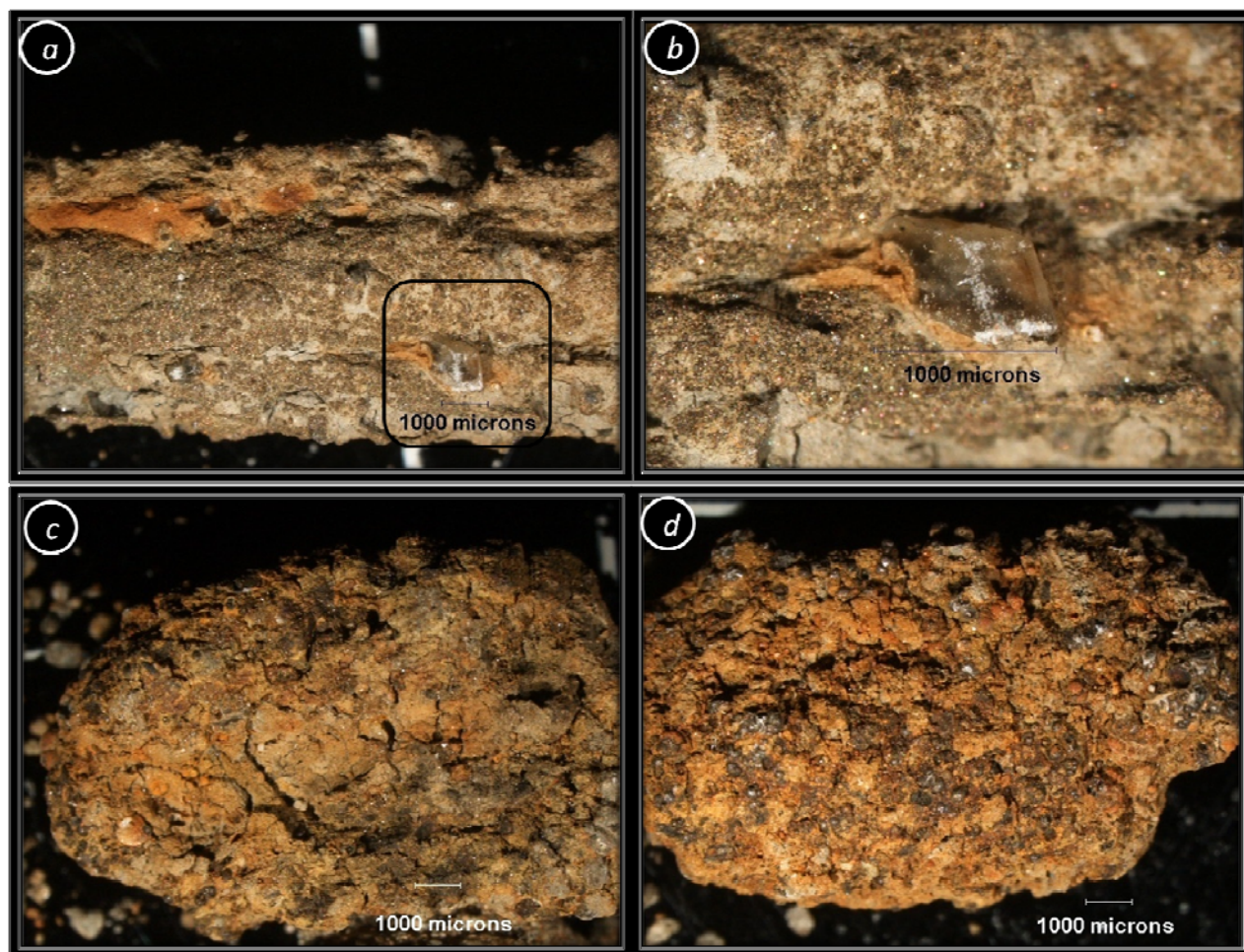


Fig.6. (a) and (b) microscopic images showing cylindrical pyrite tubules/chimneys showing protruding gypsum crystals; (c) and (d) pyrite micro nodules and gypsum crystals cemented with authigenic carbonates.

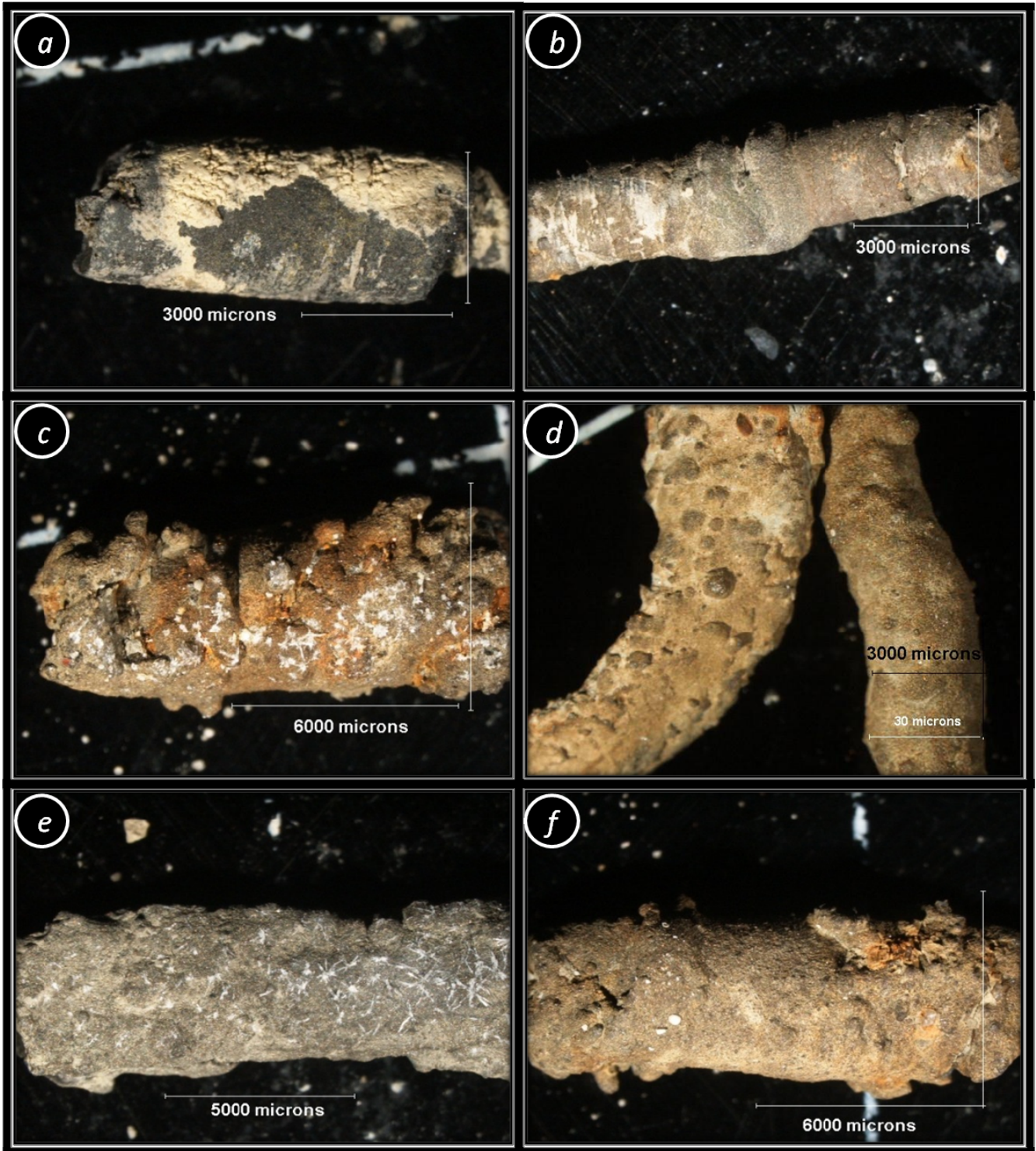


Fig.7. (a-f) microscopic images of pyrite tubules/chimneys showing different morphology

Table.1. Showing chemical compositions of different forms of gypsum crystals from SEM-EDS analysis

MD161- Site 18	Element (%)	C	Mg	Al	Si	S	K	Cl	Ca	Fe	Cu	Zn	O	Total
Rosette	Elemnt wt					24.51			26.16		0.86	0.89	47.57	100.00
	Atomic					17.30			14.77		0.31	0.31	67.30	
	Compd					SO3			CaO		CuO	ZnO		
						61.21			36.60		1.08	1.11		
Cubical	Elemnt wt			0.42	0.67	23.65		0.68	24.93	0.67	1.03	0.80	47.14	100.00
	Atomic			0.35	0.54	16.74		0.44	14.12	0.27	0.37	0.28	66.88	
	Compd			Al2O3	SiO2	SO3			CaO	FeO	CuO	ZnO		
				0.80	1.44	59.05		0.00	34.89	0.86	1.29	1.00		
Columnar	Elemnt wt			0.58	1.29	23.59			23.79	3.09			47.67	100.00
	Atomic			0.48	1.04	16.60			13.40	1.25			67.24	
	Compd			1.09	2.76	58.89			33.29	3.97				
				Al2O3	SiO2	SO3			CaO	FeO				
Irregular	Elemnt wt		0.37	1.09	2.52	22.17	0.18		23.86	2.31			47.49	100.00
	Atomic		0.34	0.91	2.02	15.55	0.10		13.39	0.93			66.67	
	Compd		MgO	Al2O3	SiO2	SO3	K2O		CaO	FeO				
			0.62	2.05	5.39	55.36	0.22		33.39	2.98				
Columnar	Elemnt wt	10.77	0.19	0.70	1.33	13.27	0.15		14.97	1.39			57.23	100.00
	Atomic	16.70	0.14	0.49	0.88	7.70	0.07		6.96	0.46			66.60	
	Compd	CO <sub>2</sub>	MgO	Al <sub>2</sub> O <sub>3</sub>	SiO <sub>2</sub>	SO <sub>3</sub>	K <sub>2</sub> O		CaO	FeO				
		39.48	0.31	1.33	2.84	33.13	0.18		20.95	1.79				
Intergrowths	Elemnt wt					24.91			27.02				48.07	100.00
	Atomic					17.43			15.13				67.43	
	Compd					SO <sub>3</sub>			CaO					
						62.19			37.81					
Lenticular	Elemnt wt			0.27	0.50	24.19			26.55	0.67			47.82	100.00
	Atomic			0.22	0.40	16.97			14.90	0.27			67.23	
	Compd			Al <sub>2</sub> O <sub>3</sub>	SiO <sub>2</sub>	SO <sub>3</sub>			CaO	FeO				
Bladed	Elemnt wt	12.62				13.20			14.86				59.32	100.00
	Atomic	18.97				7.43			6.69				66.91	
	Compd	CO <sub>2</sub>				SO <sub>3</sub>			CaO					
		46.26				7.43			20.79					

Table.2. Location of sediment cores, water depth, core length and Gypsum, Pyrite and Carbonate sub-surface distribution in sediment cores from K-G & Mahanadi offshore regions, East coast of India (\*\* based on the pore water measurement data; \* based on the authigenic carbonate distribution).

MD-161 Site no	Offshore region	Latitude(N)	Longitude(E)	Water depth (m)	Core length (m)	Gypsum, Pyrite and Carbonate distribution in different sub-surface levels (m)	SMI depth (m)
17	KG Basin	19 13.990 N	85 <sup>o</sup> 37.469' E	790	30.00	24.97-25.92	*24.97
18	Northern KG Basin	17 26.310 N	83 <sup>o</sup> 49.950' E	1691	32.00	12.03-32.00	*12.00
26	Mahanadi	19 13.9900 N	85 <sup>o</sup> 37.469'E	414	34.23	7.10-29.62	*11.21
21	Mahanadi	19 05.387 N	85 <sup>o</sup> 35.996' E	986	36.37	19.65-32.66	*19.65
22	Mahanadi	19 09.000 N	85 <sup>o</sup> 46.390' E	1365	32.40	15.50-26.00	*15.00
25	Mahanadi	19 01.810 N	85 <sup>o</sup> 38.349' E	1429	39.18	23.21-37.79	**22.30
19	Mahanadi	18 59.109 N	85 <sup>o</sup> 41.166' E	1480	39.08	11.21-39.08	**17.80
24	Mahanadi	19 03.482 N	85 <sup>o</sup> 45.841' E	1578	31.89	15.27-28.66	*16.89
23	Mahanadi	19 06.250 N	85 <sup>o</sup> 50.150' E	1600	38.62	17.25-31.80	*17.25
27	Mahanadi	18 57.360 N	85 <sup>o</sup> 43.440' E	1691	36.06	35.6-31.30	**18.62
20	Mahanadi	18 47.360 N	85 <sup>o</sup> 36.440' E	1866	50.08	22.44-47.28	*17.17